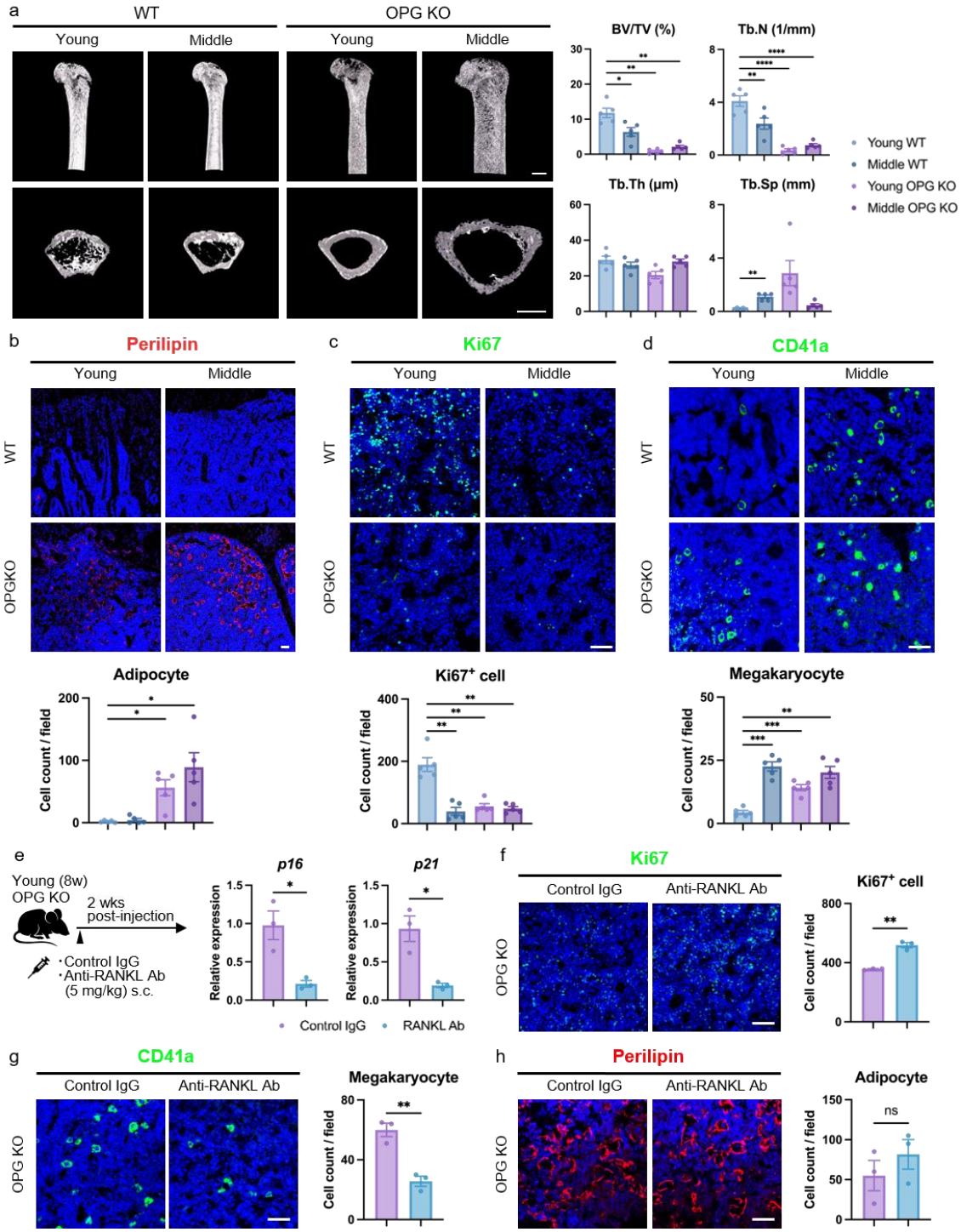

1 **Extended Data Fig. 1 Age-associated bone phenotypes in OPG KO mice**

2 **a,** μCT analysis of trabecular bone parameters in femora from young and middle-aged WT and

3 OPG KO mice. *n* = 5 biological replicates. Scale bar, 1 mm.

4 **b–d,** Immunofluorescence of Perilipin$^+$ (**b**), Ki67$^+$ (**c**), and CD41a$^+$ (**d**) cells in bone marrow

from young and middle-aged WT and OPG KO mice. $n = 5$ biological replicates. Scale bar, 50 μm.

e, Quantitative RT–PCR analysis of *p16* and *p21* expression in young OPG KO mice treated with anti-RANKL antibody or control IgG. $n = 3$ biological replicates.

f–h, Immunofluorescence of $Ki67^+$ (**f**), $CD41a^+$ (**g**), and $Perilipin^+$ (**h**) cells in femora from young OPG KO mice treated with anti-RANKL antibody or control IgG. $n = 3$ biological replicates. Scale bar, 50 μm.

a–h, Data are presented as mean ± s.d. Statistical significance was determined using Brown–Forsythe and Welch ANOVA followed by Dunnett's T3 multiple-comparisons test or unpaired two-tailed Welch's *t*-test (*P < 0.05, **P < 0.01, ***P < 0.001, ****P < 0.0001, ns, not significant).

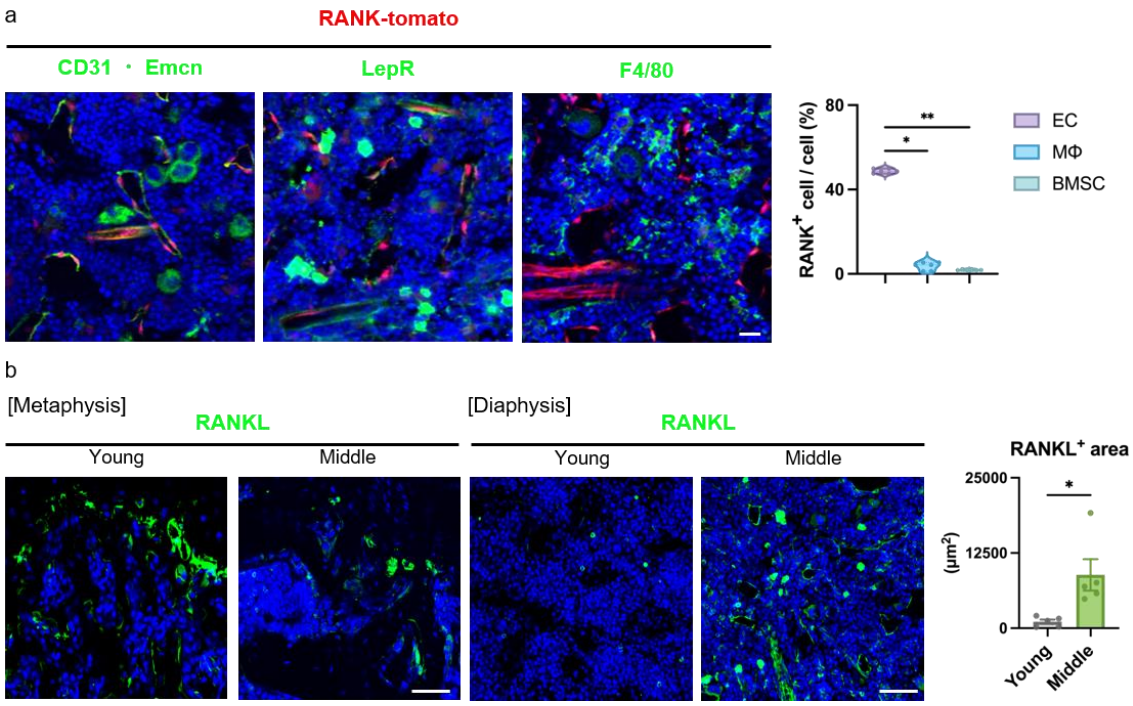

Extended Data Fig. 2 RANK⁺ endothelial cells are increased in middle-aged bone marrow

a, Immunofluorescence of femora from middle-aged RANK-tom mice stained for CD31 and Emcn, F4/80, and LepR. $n = 5$ biological replicates. Scale bar, 50 μm.

b, RANKL immunofluorescence in femora from young and middle-aged WT mice. $n = 5$ biological replicates. Scale bar, 50 μm.

a, Data are presented as median with interquartile range. Statistical significance was determined using the Kruskal–Wallis test followed by Dunn's multiple-comparisons test (*P < 0.05, **P < 0.01).

b, Data are presented as mean ± s.d. Statistical significance was determined using unpaired two-tailed Welch's *t*-test (*P < 0.05).

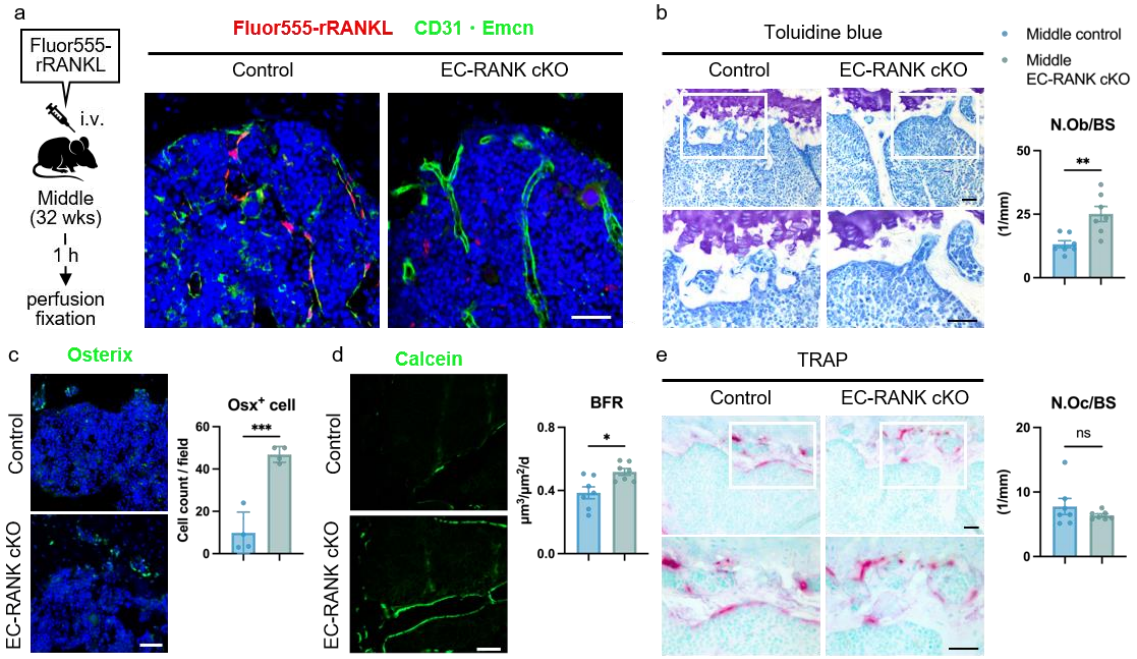

28 **Extended Data Fig. 3 Depletion of endothelial Rank improves aging-associated**

29 **decline in bone formation**

30 **a,** Immunofluorescence of CD31 and Emcn in femora from middle-aged control and EC-RANK

31 cKO mice after intravenous injection of Fluor555-rRANKL. *n* = 3 biological replicates. Scale

32 bar, 50 μm.

33 **b,** Toluidine blue staining of tibial sections from middle-aged control and EC-RANK cKO

34 mice. *n* = 7 biological replicates. Scale bar, 50 μm.

35 **c,** Osterix immunofluorescence in femora from middle-aged control and EC-RANK cKO mice.

36 *n* = 4 biological replicates. Scale bar, 50 μm.

37 **d,** Calcein double labeling of tibiae to determine bone formation rate. *n* = 7 biological

38 replicates. Scale bar, 50 μm.

39 **e,** TRAP staining of tibiae from middle-aged control and EC-RANK cKO mice. *n* = 7 biological

replicates. Scale bar, 50 μm.

b–e, Data are presented as mean ± s.d. Statistical significance was determined using unpaired two-tailed Welch's *t*-test (*P < 0.05, **P < 0.01, ns, not significant).

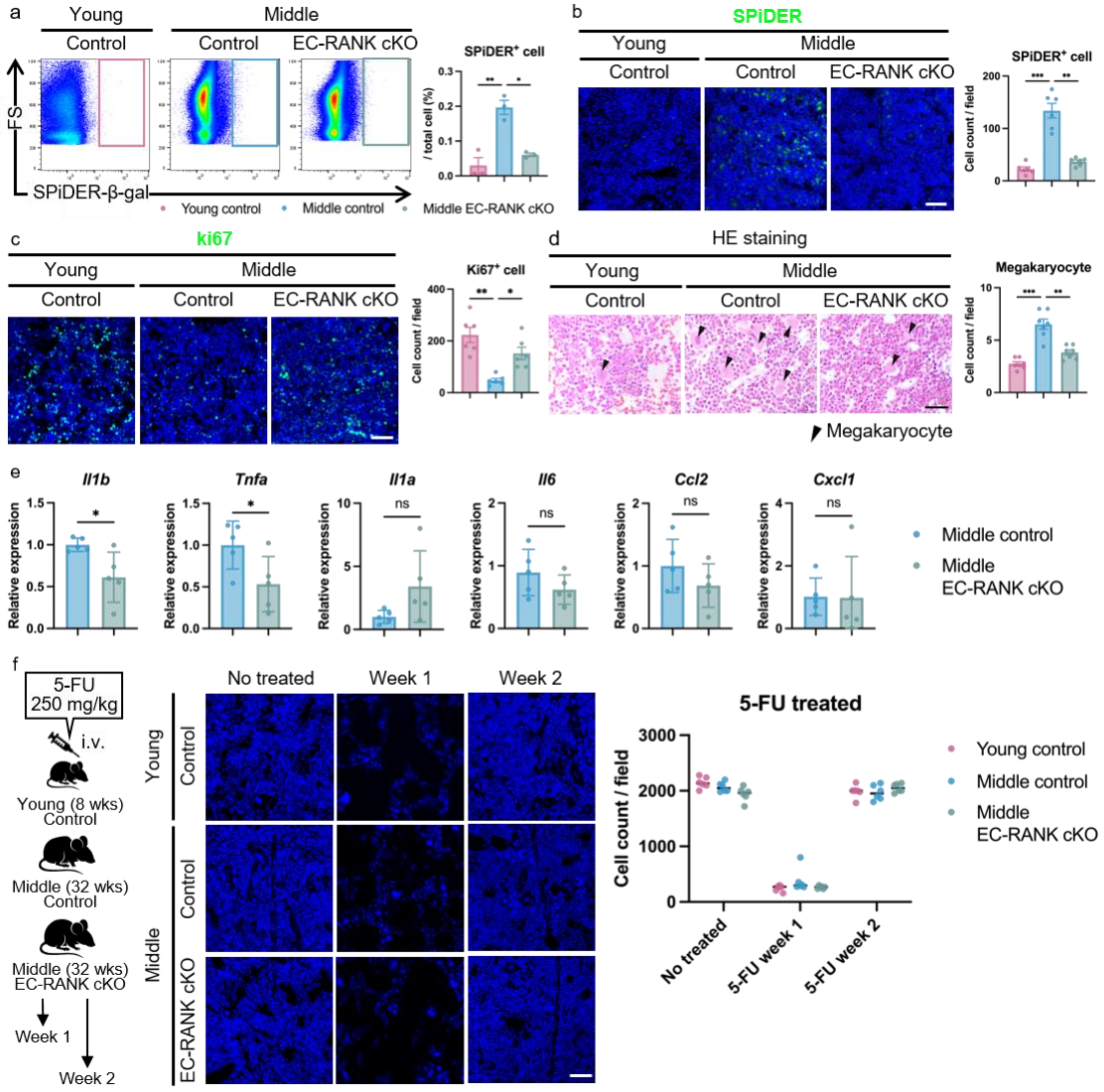

Extended Data Fig. 4 Deletion of endothelial Rank restores aging-associated senescent cell accumulation and aberrant HSC output

a, Flow cytometry analysis of SPiDER-β-gal$^+$ cells in bone marrow from young and middle-aged control and EC-RANK cKO mice. n = 3 biological replicates.

b, SPiDER-β-gal staining in femora from young and middle-aged control and EC-RANK cKO mice. n = 6 biological replicates. Scale bar, 50 μm.

c, Ki67 immunofluorescence in femora from middle-aged control and EC-RANK cKO mice. n = 6 biological replicates. Scale bar, 50 μm.

d, Hematoxylin and eosin-stained tibial sections from middle-aged control and EC-RANK cKO mice. $n = 7$ biological replicates. Scale bar, 50 μm.

e, Quantitative RT–PCR analysis of SASP gene expression in tibiae from middle-aged control and EC-RANK cKO mice. $n = 5$ biological replicates.

f, Quantification of bone marrow cellularity in femora from young and middle-aged control and middle-aged EC-RANK cKO mice before and 1 or 2 weeks after intravenous administration of 5-FU (250 mg/kg). n = 6 biological replicates.

a–e, Data are presented as mean ± s.d. Statistical significance was determined using Brown–Forsythe and Welch ANOVA followed by Dunnett's T3 multiple-comparisons test or unpaired two-tailed Welch's *t*-test (*P < 0.05, **P < 0.01, ***P < 0.001, ns, not significant).

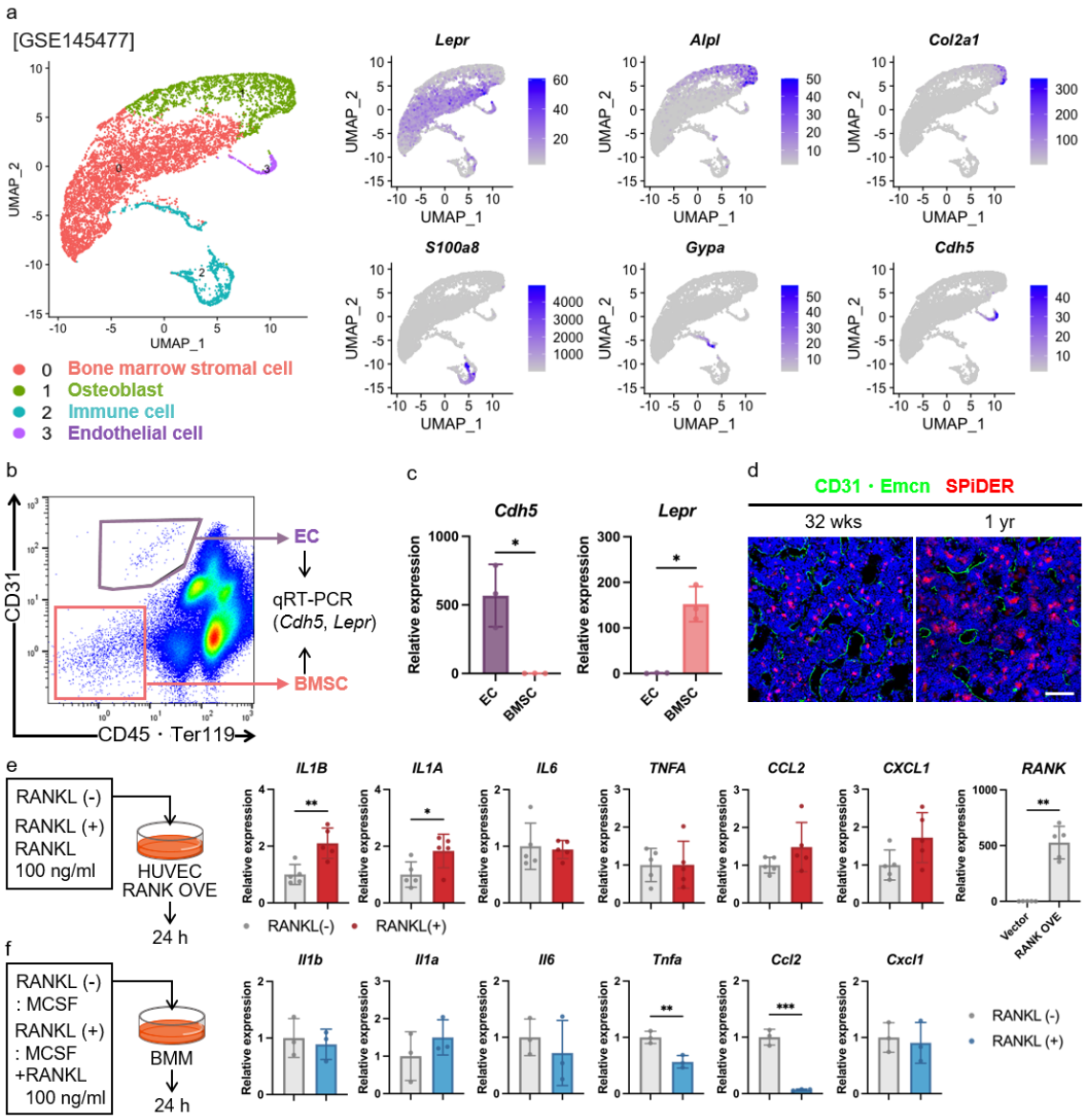

Extended Data Fig. 5 Characterization of endothelial cells by scRNA-seq and FACS analysis, and effects of RANKL on IL-1β and SASP expression

a, UMAP visualization of reanalyzed scRNA-seq data (GSE145477) from bone marrow of 16-month-old mice. Feature plots show expression of canonical marker genes in BMSCs, osteoblasts, immune cells, and endothelial cells.

b,c, Cell sorting of endothelial cells ($CD31^+CD45^-Ter119^-$) and stromal cell-rich fractions ($CD31^-CD45^-Ter119^-$), and quantitative RT–PCR analysis of *Cdh5* and *Lepr* expression. $n = 3$

biological replicates.

d, CD31and Emcn immunofluorescence and SPiDER-β-gal staining in femora. $n = 6$ biological replicates. Scale bar, 50 μm.

e, Quantitative RT–PCR analysis of SASP gene expression in HUVECs transfected with *Tnfrsf11a* or control vector and treated with RANKL (100 ng/mL) for 24 h. $n = 5$ biological replicates.

f, Quantitative RT–PCR analysis of SASP gene expression in bone marrow macrophages treated with RANKL (100 ng/mL) for 24 h or untreated. $n = 3$ biological replicates.

b–f, Data are presented as mean ± s.d. Statistical significance was determined using unpaired two-tailed Welch's *t*-test (*P < 0.05, **P < 0.01).

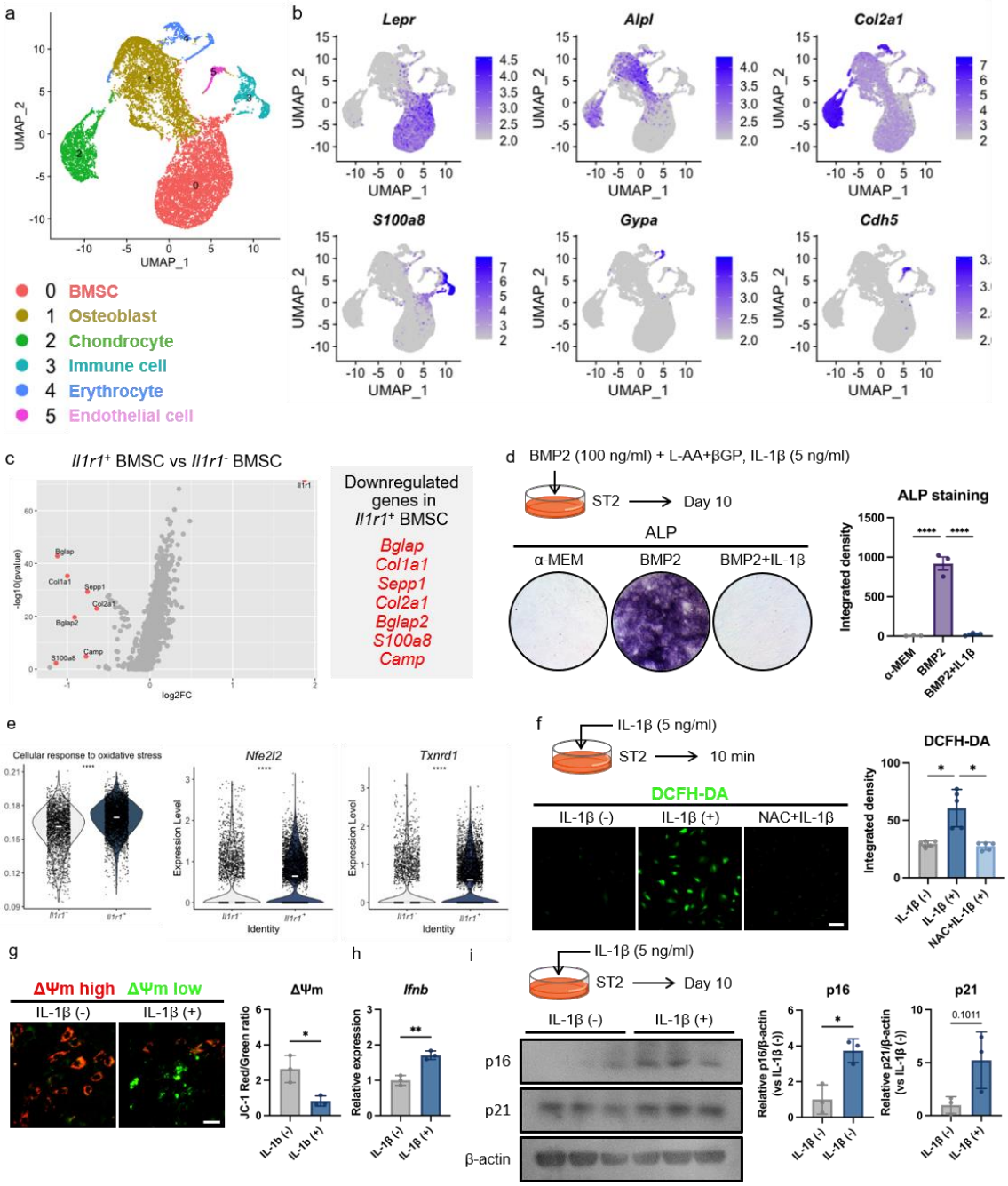

Extended Data Fig. 6 Identification of Il1r1-expressing clusters and effects of IL-1β on senescence

a, UMAP visualization of scRNA-seq data from bone marrow of 1.5-month-old and 16-month-old mice.

b, Feature plots showing expression of canonical marker genes.

c, Volcano plot showing DEGs between *Il1r1*$^{+}$ and *Il1r1*$^{-}$ BMSCs.

d, Alkaline phosphatase staining and quantification of alkaline phosphatase (ALP) activity. n = 3 biological replicates.

e, Violin plots showing ROS-related pathway activity and representative oxidative stress response genes in *Il1r1*$^{-}$ and *Il1r1*$^{+}$ BMSCs. The left panel shows the UCell score for the GO cellular response to oxidative stress pathway, and the right panels show expression levels of *Nfe2l2* and *Txnrd1*. Each dot represents one cell. White horizontal bars indicate the median.

f, Representative images of DCFH-DA staining in ST2 cells treated with IL-1β with or without N-acetylcysteine (NAC) for 10 min. Quantification of intracellular ROS levels by integrated density (IntDen) is shown. n = 5 biological replicates. Scale bar, 50 μm.

g, Representative images of JC-1 staining in ST2 cells treated with IL-1β. Quantification of the JC-1 red/green fluorescence intensity ratio by ROI analysis of individual cells is shown. Red and green fluorescence indicate high and low mitochondrial membrane potential (ΔΨm). Values represent the mean of all analyzed cells. n = 3 biological replicates. Scale bar, 50 μm.

h, Quantitative RT-PCR analysis of Ifnb expression in ST2 cells treated with or without IL-1β. n = 3 biological replicates.

i, Representative western blots of p16 and p21 in ST2 cells treated with IL-1β for 10 days. Quantification of p16 and p21 protein expression normalized to β-actin is shown. n = 3 biological replicates.

d-i, Data are presented as mean ± s.d. Statistical significance was determined by one-way ANOVA followed by Dunnett's multiple-comparisons test (d, f), Wilcoxon rank-sum test (e), unpaired two-tailed Welch's t-test (g-i). (*$p < 0.05$; **$p < 0.01$; ****$p < 0.0001$).